Available online at www.sciencedirect.com
ScienceDirect
Trans. Nonferrous Met. Soc. China 32(2022) 2229−2242
Transactions of Nonferrous Metals Society of China
www.tnmsc.cn

Microstructural evolution and mechanical properties of forged β-solidified γ-TiAl alloy by different heat treatments

Xiao-bing LI[1], Hao XU[2], Wei-wei XING[3], Bo CHEN[1], Lei SHU[1], Meng-shu ZHANG[1], Kui LIU[1]

1. Ji Hua Laboratory (Advanced Manufacturing Science and Technology Guangdong Laboratory), Foshan 528200, China;
2. MIIT Key Laboratory of Advanced Metallic and Intermetallic Materials Technology, Nanjing University of Science and Technology, Nanjing 210094, China;
3. Shi-changxu Innovation Center for Advanced Materials, Institute of Metal Research, Chinese Academy of Sciences, Shenyang 110016, China

Received 9 July 2021; accepted 18 December 2021

Abstract: The microstructural evolution and tensile properties of a forged Ti−42Al−5Mn alloy subjected to different heat treatments were studied. The results showed that, when the forged alloy was aged at 800 °C for 24 h, the interlamellar spacing (λ) and γ grain size at colony boundaries are generally coarsened. Whereas, when the alloy was first annealed at 1300 °C and then aged at 800 °C for 24 h, this coarsening of related microstructures appears less pronounced. The suggested annealing temperatures for the forged Ti−42Al−5Mn alloy are in the range of 1250−1300 °C. It was found that, on the condition of the same annealing system, both the strength and ductility were improved as the aging temperature changed from 1000 to 800 °C. The secondary precipitated β_o ($\beta_{o,sec}$) at colony boundaries could be responsible for improving the strength, and the γ phase at colony boundaries with the grain size about 6 μm might be one of the main reasons for the better ductility.

Key words: β-solidifying γ-TiAl alloy; forge; heat treatment; microstructural evolution; mechanical properties

1 Introduction

Gamma-titanium aluminide (γ-TiAl) has been considered as the topmost candidate for high-temperature structural material because of its low density and high specific modulus and strength [1−5]. Unfortunately, the intricate processing procedures, which are greatly due to the intrinsic brittleness and poor hot workability, appear to be the main obstacles for a wide industrial application of γ-TiAl alloys [5,6]. The β-solidified γ-TiAl alloys (via β-phase solidification), proposed by NAKA et al [7] and called as beta solidified gamma (BSG) alloys by KIM and KIM [8], arouse increasing attention due to their suitable workability and appropriate solidification process without any peritectic segregation [9,10].

In general, the BSG alloys are with one or more β stabilizing elements, such as Mo, Cr, Mn, V, Nb, and lower Al content (42%−44%) compared to conventional gamma (CG) alloys [8,11]. There are two typical BSG alloys, namely Ti−42Al−5Mn developed by TETSUI et al [12] and Ti−43Al−4Nb−1Mo−0.1B (TNM) proposed by CLEMENS et al [13]. TNM alloy contains certain amount of refractory alloying elements, such as Nb and Mo, which would in turn increase the difficulty of melting and hot processing [13−17]. The available literature showed that TNM alloy needed to experience multiple vacuum arc remelting (VAR) many times to achieve adequate chemical and

Corresponding author: Bo CHEN, E-mail: chenbo@jihualab.ac.cn
DOI: 10.1016/S1003-6326(22)65943-0

structural homogeneity [18]. As for the forging process, high temperature (above 1300 °C) isothermal and canned forging must be adopted [19], i.e, it is usually encapsulated in thick stainless steel cans or titanium alloy cans and forged at constant high temperature due to its limited hot workability.

As for Ti−42Al−5Mn alloy, it indeed has the advantage of low cost and great deformability. Our previous research has confirmed that this alloy can be hot-worked from 1300 °C, 10 s^{-1} to 1100 °C, 0.1 s^{-1} [20], whose processing window is significant wider than that of TNM alloy [21,22]. It means that the conventional forging process without any extra isothermal or canned procedure could be used to manufacture this alloy [12,23]. In addition, for a fixed chemical composition alloy, multiple heat treatments are also needed to further improve its mechanical properties. Generally, the two-step heat treatments including annealing and aging treatments can be introduced to BSG alloys to optimize the microstructure according to Ref. [18]. Regrettably, since the study on Ti−42Al−5Mn alloy is still at its initial stage, the control of microstructure and mechanical properties of this alloy after forging is seldom reported.

The present work was to study the microstructural evolution and mechanical properties of the forged Ti−42Al−5Mn resulting from various two-step heat treatments (annealing and aging treatments). The effects of various microstructures including α_2/γ lamellae, γ phase, and β_o phase precipitated in the lamellar colonies on the tensile mechanical properties of the forged Ti−42Al−5Mn alloy were also systematically identified and discussed.

2 Experimental

2.1 Specimen preparation

The as-cast Ti−42Al−5Mn (42Al−5Mn) ingot with dimensions of *d*120 mm × 400 mm was prepared by vacuum induction melting (VIM) and VAR using industrially pure materials. A cylinder of *d*50 mm × 110 mm was cut from the ingot and forged into a bar with the deformation of 69% at 1300 °C by using conventional forging process without any isothermal or canned condition.

2.2 Heat treatment

The heat treatment experiments were conducted by a high temperature resistance furnace (KSL−1400X), and the temperature control error is within ±1 °C. In this section, the forged and annealed samples (1300 °C, 30 min, AC) with the sizes of *d*8 mm × 10 mm were aged at 800 °C with the holding time from 3 to 24 h. And also, some of the forged samples with the same size were subjected to different annealing treatments (see Table 1). Under the optimized annealing treatment, samples with sizes of *d*11 mm × 70 mm were then experienced various two-step heat treatments, as shown in Fig. 1. Meanwhile, to evaluate the grain coarsening potential, one of the heat treatments reduced the holding time from 30 to 10 min (HT #7).

Table 1 Annealing treatment schemes of forged Ti−42Al−5Mn samples

Annealing treatment	Phase region at annealing temperature [24]
1350 °C, 30 min, AC	β
1300 °C, 30 min, AC	$\beta+\alpha(\sim T_\beta)$
1250 °C, 30 min, AC	$\beta+\alpha$
1200 °C, 30 min, AC	$\beta+\alpha+\gamma$
1150 °C, 30 min, AC	$\beta+\alpha_2+\gamma(\sim T_{\gamma,\mathrm{solv}})$
1100 °C, 30 min, AC	$\beta+\alpha_2+\gamma$

Note: AC is air cooling

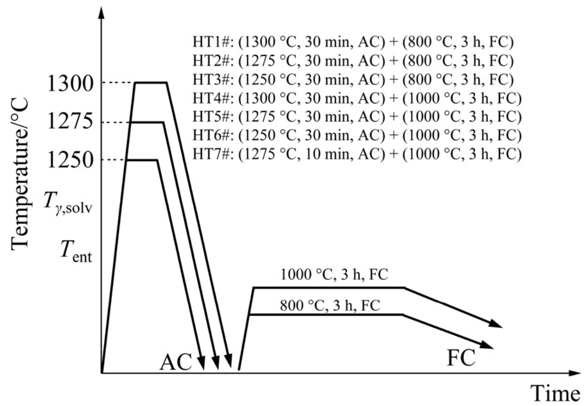

Fig. 1 Forged samples under different heat treatments (FC is furnace cooling)

2.3 Metallographic observations

The microstructures under different heat treatment conditions were characterized by field emission electron probe microanalyzer (EPMA) in back scattered electron mode (BSE) with a JXA−8530F. The detail microstructure information of α_2/γ lamellae in these samples was further analyzed by transmission electron microscopy (TEM) (Tecnai G^2 20). TEM-samples were prepared with special reagent (60% methyl alcohol + 30% *N*-butyl alcohol + 10% perchloric acid) by twin-jet machine. The interlamellar spacing (λ) and γ grain size as well as the volume fraction of different structures were characterized using a professional image analysis software (Image Pro Plus 6.0). For each sample, more than six visual fields were captured and the values were averaged based on the image analysis software.

2.4 Tensile tests

The samples underwent the two-step heat treatments were machined into tensile specimens with a gauge diameter of 5 mm and a length of 30 mm according to GB/T 228.1—2010 standard. Tensile testing was performed on a universal testing machine MTS E45.105. The yield strength ($R_{p0.2}$), tensile strength (R_m), and elongation (A) at room temperature (RT) were obtained in the tensile test.

3 Results

3.1 As-forged microstructure

The as-forged microstructure of Ti−42Al−5Mn alloy is shown in Fig. 2. It is a typical nearly lamellar (NL) microstructure, which mainly consists of bright β_o phases, dark γ phases and equiaxed α_2/γ lamellae (arrows in Fig. 2(b)). The average lamellar colony size is about 40 μm, and that of γ grains at the colony boundaries is approximately 4.42 μm. As can be seen from Fig. 2(c), the lamellar colony is composed of γ and α_2 phases, with an average lamellar spacing of 189 nm.

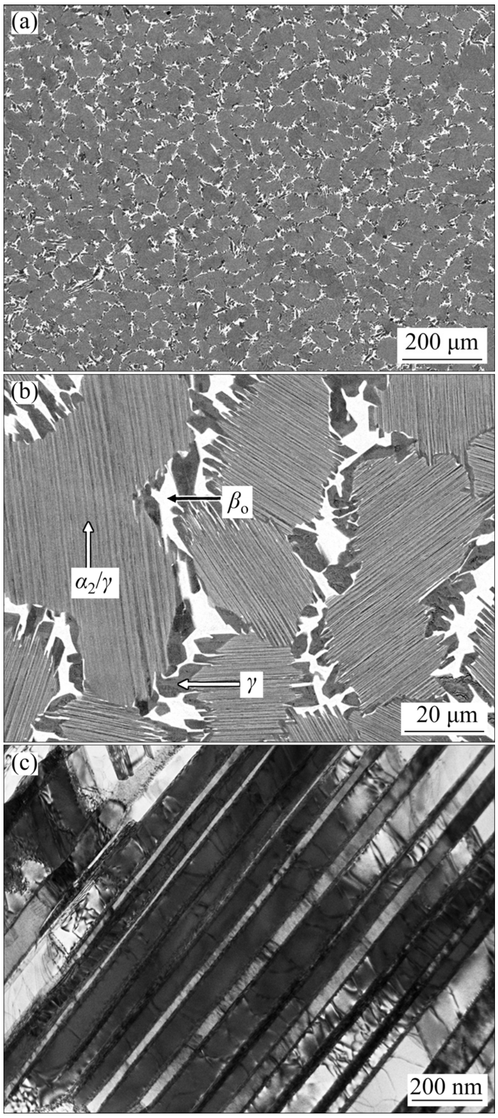

Fig. 2 Microstructures of as-forged Ti−42Al−5Mn alloy: (a, b) EPMA images in BSE mode; (c) TEM image of lamella

3.2 Microstructure of forged Ti−42Al−5Mn in different aging periods

Figure 3 presents the microstructures of forged Ti−42Al−5Mn alloy after aging at 800 °C. Figure 4 shows the TEM images of lamellar structure in these aged samples. It can be found that after aging at 800 °C for 24 h, the microstructure is still a typical NL microstructure. According to Table 2, as the aging time increases to 24 h, the λ is significantly increases from 189 nm (0 h) to 640 nm (24 h), and the γ grain size is also coarsened from 4.42 μm (0 h) to 6.39 μm (24 h), whereas the average size of the α_2/γ-colonies changes little. It suggests that the lamellar structure and γ grain obtained from the forging process will be coarsened in the following 800 °C aging.

3.3 Microstructure of annealed Ti−42Al−5Mn in different aging periods

Figure 5 shows microstructures of the annealed Ti−42Al−5Mn after aging at 800 °C. Figure 6 illustrates the TEM images of lamellar structure for these aged samples. Based on the quantitative analysis results shown in Table 3, after 1300 °C annealing treatment, the λ size is refined from 189 to 103 nm, meanwhile the γ grain size is refined from 4.42 to 2.29 μm in comparison with the forged microstructure. However, the size of

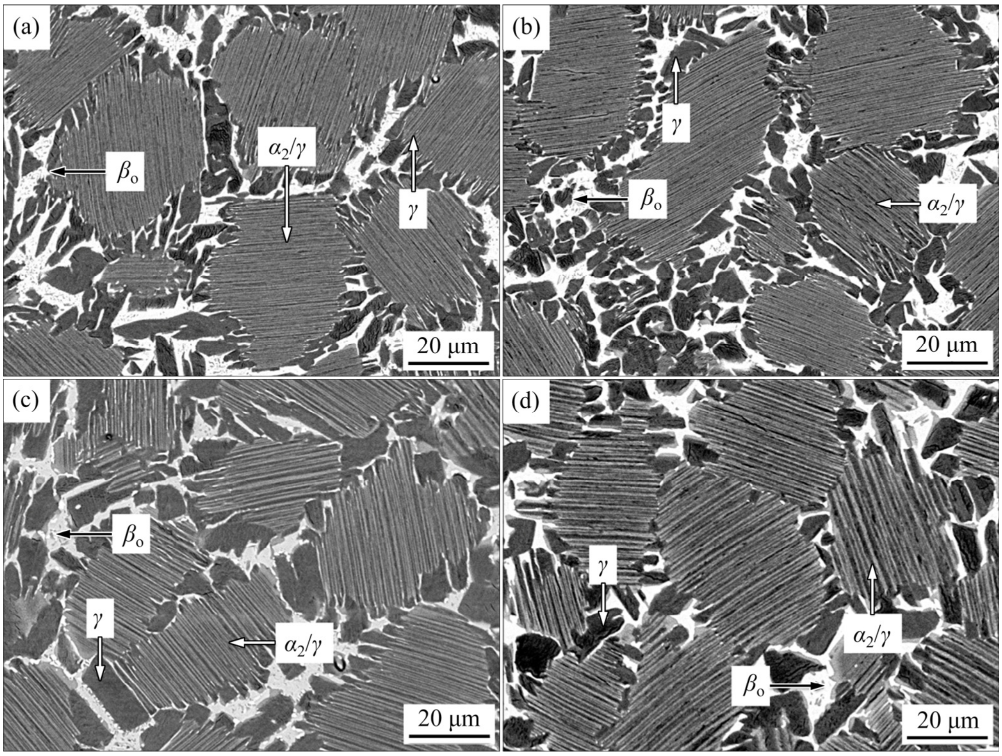

Fig. 3 Microstructures of as-forged Ti−42Al−5Mn alloy treated for different aging time: (a) 3 h; (b) 6 h; (c) 12 h; (d) 24 h

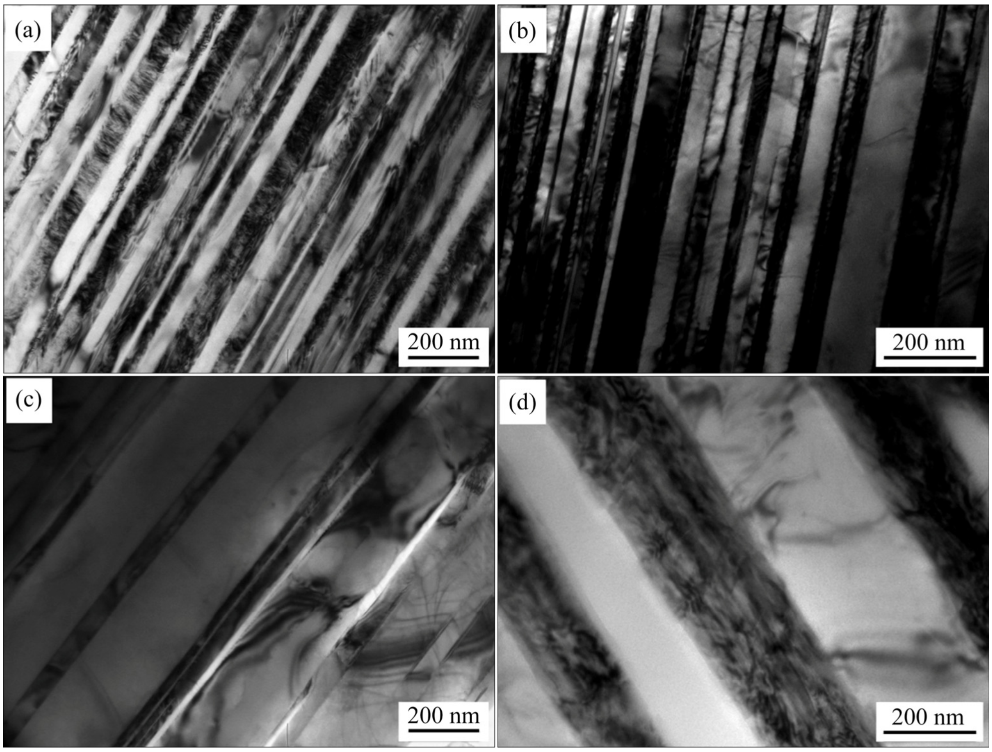

Fig. 4 TEM images of α_2/γ lamellae aged for different time: (a) 3 h; (b) 6 h; (c) 12 h; (d) 24 h

α_2/γ-colonies and γ grain did not significantly change with increasing the aging time from 3 to 24 h. Although λ is increased from 103 nm (0 h) to 163 nm (24 h), the increment is obviously lower than that of forged specimen. It indicates that the annealing treatment at 1300 °C has a positive effect on improving the stability of the forged microstructure during exposure at 800 °C.

Table 2 Microstructural parameters of as-forged and aged alloys

Aging time/h	Type of microstructure	Phase fraction/%			Average size/μm		λ/nm
		γ	β_o	α_2/γ	γ	α_2/γ colony	
0(as-forged)	NL	17.55	12.70	69.75	4.42	36.78	189
3	NL	19.13	11.83	69.04	4.72	34.62	210
6	NL	20.18	11.44	68.38	4.75	34.52	233
12	NL	24.51	10.45	65.04	6.12	33.79	486
24	NL	25.85	9.51	64.64	6.39	33.63	640

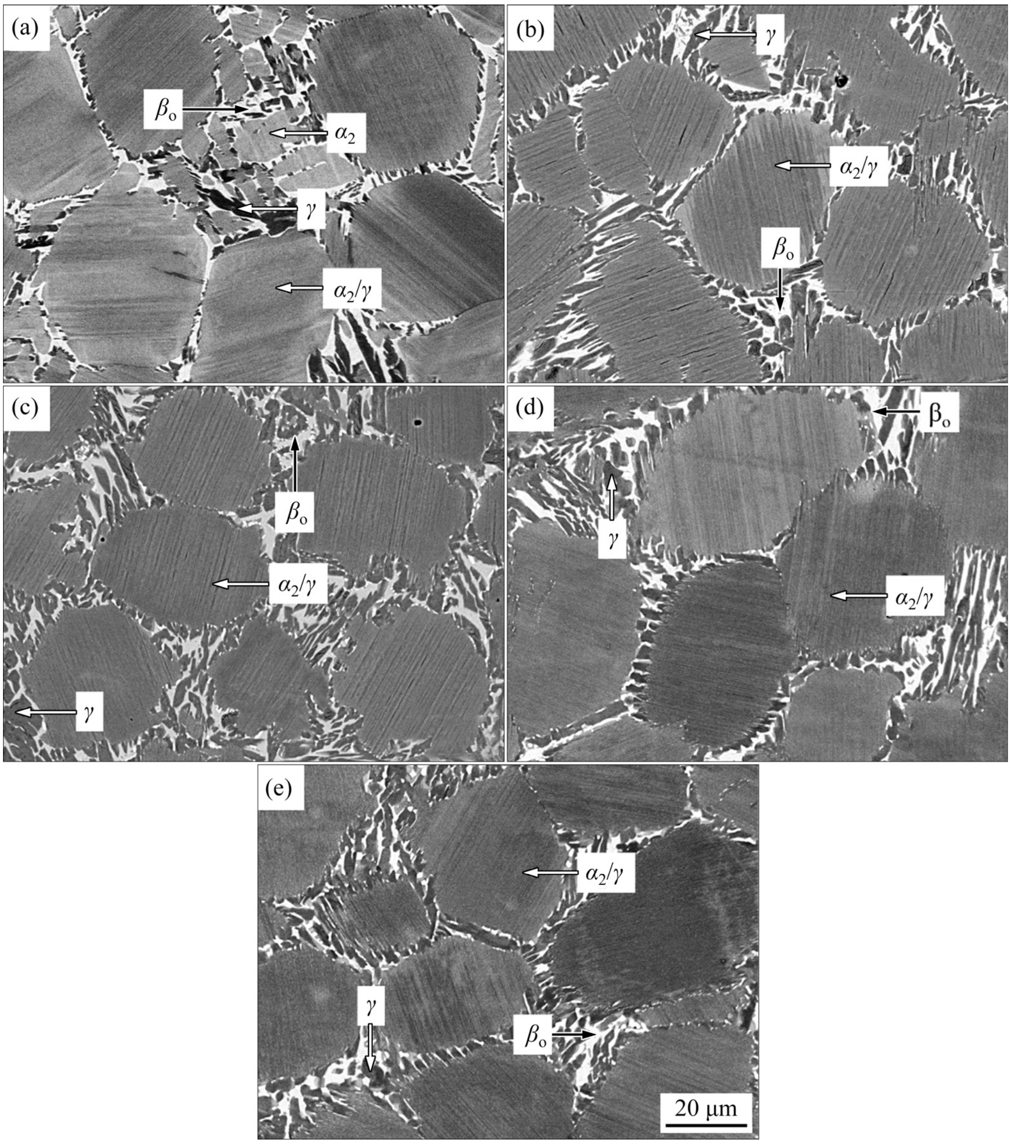

Fig. 5 Microstructures of samples annealed at 1300 °C in different aging periods: (a) 0 h; (b) 3 h; (c) 6 h; (d) 12 h; (e) 24 h

3.4 Microstructures of forged Ti−42Al−5Mn subjected to different annealing treatments

The above results confirm that the thermal stability of forged Ti−42Al−5Mn alloy can be improved by 1300 °C annealing treatment. In order to optimize the annealing treatment, it is necessary to clarify the effect of the annealing temperature on the microstructure evolution of this alloy.

Figure 7 shows the microstructures of the as-forged Ti−42Al−5Mn alloy after subjecting to

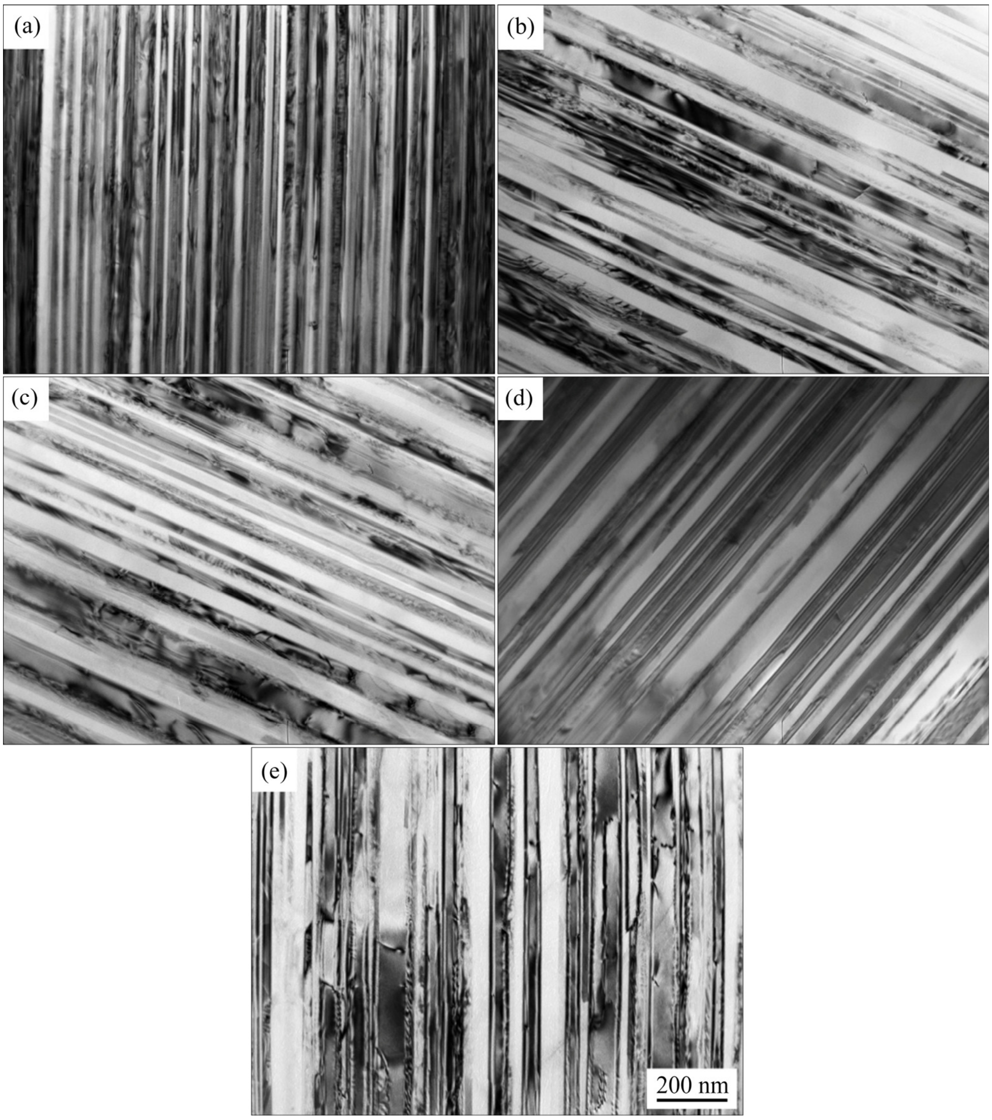

Fig. 6 TEM images of α_2/γ lamellae in annealed samples under different aging periods: (a) 0 h; (b) 3h; (c) 6 h; (d) 12 h; (e) 24 h

Table 3 Microstructural parameters of as-forged and 1300 °C annealed alloys under different aging periods

Aging time/h	Type of microstructure	Phase fraction/%			Average size/μm		λ/nm
		γ	β_o	α_2/γ	γ	α_2/γ colony	
As-forged	NL	17.55	12.70	69.75	4.42	36.78	189
0	NL	7.76	8.74	83.50	2.29	36.74	103
3	NL	13.22	9.04	77.74	3.05	34.35	134
6	NL	14.33	8.54	77.13	3.03	34.16	135
12	NL	13.94	8.34	77.72	3.00	36.63	145
24	NL	12.97	8.83	78.20	3.23	34.92	163

different annealing treatments. Table 4 shows the microstructural parameters of as-forged and annealed alloys. As can be seen from Fig. 7(a), when the annealing temperature is 1350 °C, the microstructure consisted of α_2/γ lamellae, γ grain, β_o phase and a few supersaturated α_2 phases. The equiaxed α_2/γ lamellae obtained from the forging process disappear, and the α_2/γ colony is

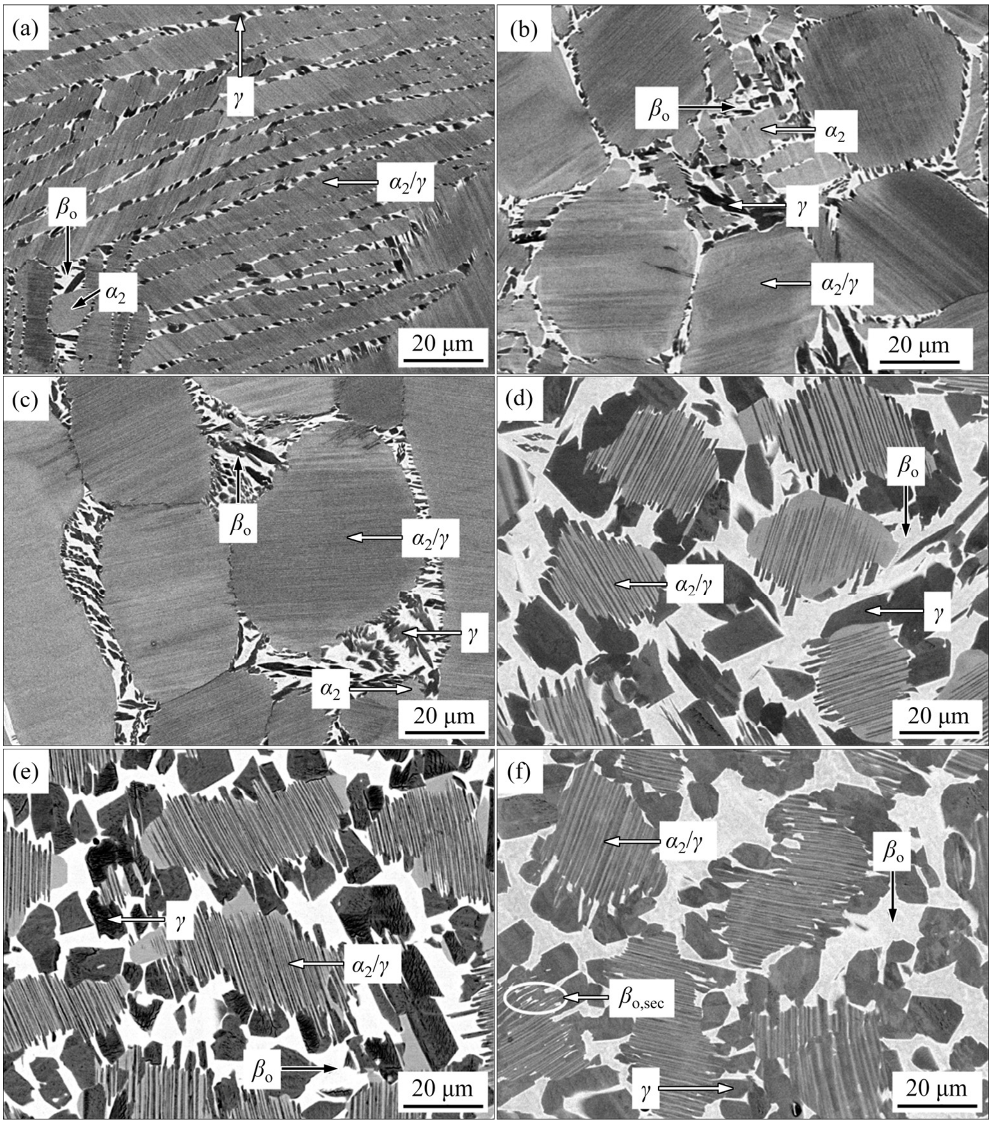

Fig. 7 Microstructures of forged Ti−42Al−5Mn alloy after subjecting to different annealing treatments at 1350 °C (a), 1300 °C (b), 1250 °C (c), 1200 °C (d), 1150 °C (e), and 1100 °C (f)

Table 4 Microstructural parameters of as-forged and annealed alloys

Solution temperature/°C	Phase fraction/%			Average size/μm	
	γ	β_o	α_2/γ	γ	α_2/γ colony
As-forged	17.55	12.70	69.75	4.42	36.78
1350	7.66	4.95	87.39	1.74	−
1300	7.76	8.74	83.50	2.29	36.74
1250	8.30	9.87	81.83	2.43	37.24
1200	36.73	26.03	37.24	7.02	23.33
1150	35.76	24.60	38.64	7.22	25.57
1100	36.39	25.34	38.27	7.33	22.27

significantly elongated. It should be mentioned that the γ grain is refined from 4.42 to 1.74 μm compared with the as-forged sample (see Table 4). It is also found that the volume fraction of α_2/γ lamellae is increased to 87.39% and that of β_o phase is reduced to 4.95% by 1350 °C annealing treatment.

According to Table 1, just β single phase exists after treating at 1350 °C. This means that all the phases formed during forging would be completely dissolved into β phase at this temperature. When it was cooled with AC method, different phase transformations could happen, such as $\beta\rightarrow\alpha$, $\beta\rightarrow\gamma$, and $\alpha_2\rightarrow\alpha_2/\gamma$ [24]. Due to the relatively high cooling rate in air, a few supersaturated α_2 grains can be identified. It can be found that when they were re-precipitated from β phase during air cooling, γ phase tends to have a smaller size than the original one. In addition, because the alloy is completely in β-phase region, there is almost no α-phase pinning effect, and the lamellae tend to be in Widmanstätten morphology rather than equiaxed characteristic as a result of $\beta\rightarrow\alpha$ transformation at high temperature, which is similar to the as-cast microstructure [25].

When the temperature decreases to 1300 and 1250 °C (Figs. 7(b, c)), the alloy is in $\beta+\alpha$ dual-phase region with slight (1300 °C) or strong (1250 °C) α-phase pinning effects, the equiaxed α_2/γ lamellae is preserved. The size of γ grain nucleated from β phase, is similar to that of 1350 °C treated sample, and is much smaller than that of as-forged sample (see Table 4). As can be seen, the microstructure still mainly consists of α_2/γ lamellae (above 80%) when the temperature is in the range of 1250−1300 °C.

As the temperature decreases to the $\beta+\alpha+\gamma$ triple-phase region (1200−1100 °C), there is some difference among the three samples (1200, 1150, 1100 °C). When the annealing temperatures are 1200 and 1150 °C (Figs. 7(d, e)), most of the α phases are transformed into α_2/γ lamellae, but there still exist a few supersaturated α_2 phases. When the temperature is 1100 °C (Fig. 7(f)), few supersaturated α_2 phases can be characterized because the α_2/γ lamellae cannot transform into α_2 phases at this temperature [24]. Besides, a small amount of dotted β_o phases can be observed in the lamellar colonies. To differentiate these dotted β_o phases and the irregular β_o phases, we name these dotted β_o phases as the second precipitated β_o phases ($\beta_{o,sec}$), which were proved to be the reaction products of $\alpha_2/\gamma\rightarrow\beta_{o,sec}$. Detailed information on the $\beta_{o,sec}$ can be found in our previous research [26]. As seen in Table 4, in comparison with the samples annealed at 1250−1350 °C, the volume fraction of α_2/γ lamellae is plummeted to ~38%, while that of β_o is raised sharply to ~25%. Also, significant increase of the volume fraction and average size of γ grain is found in these three samples.

3.5 Microstructure and tensile properties of as-forged Ti−42Al−5Mn subjected to two-step heat treatments

As discussed above, to obtain fine microstructure, the annealing temperature should be selected as 1250−1300 °C. Usually, the BSG alloys experience two-step heat treatment, including annealing and aging treatments, to obtain excellent mechanical properties such as high strength and good ductility. In this work, the as-forged alloy was then subjected to different heat treatments (in Section 2.2) to understand the influence of two-step heat treatments on tensile properties.

Figure 8 illustrates the microstructure characteristics of the as-forged Ti−42Al−5Mn alloy subjected to different heat treatments. The tensile properties are shown Table 5. As can be seen in Figs. 8(a−c), after aging at 800 °C, the microstructure mainly consists of equiaxed α_2/γ lamellae, γ grains and β_o phase at colony boundary. For 1000 °C aging samples (Figs. 8(d−g)), besides the $\alpha_2/\gamma+\gamma+\beta_o$ microstructures, plenty of $\beta_{o,sec}$ phases can also be detected at lamellar interfaces.

Combined with the tensile properties (see Table 5 and Fig. 9), it is seen that for the samples aged at 800 °C, the yield strengths are all around 520 MPa and the elongation is generally less than 0.5% with the annealing temperature from 1300 to 1250 °C. When aged at 1000 °C, the yield strength increases from 636 to 704 MPa and the elongation decreases from 0.80% to 0.29% with the temperature from 1300 to 1250 °C. After further reducing the time to 10 min, the yield strength is increased to 735 MPa and the elongation is maintained at 0.55%.

It is found that the changes in the tensile properties of samples with different annealing treatments are not obvious among the 800 °C aging samples. Whereas, for 1000 °C aging specimens, with the decrease of annealing temperature, the strength of the alloy is obviously increased and the ductility is slightly reduced. From Table 5, the γ grain sizes in the HT#1 to HT#3 samples remain at ~3 μm and the α_2/γ-colonies size remains at ~36 μm. Previous research [27] has confirmed that the size of γ grain and α_2/γ-colonies are the major determinants for tensile properties of γ-TiAl alloy. Because of this, the RT tensile properties of the three samples show no significant change. Under the condition of 1000 °C aging, although the γ grain size in these samples keeps at ~6 μm, the α_2/γ-colonies size in HT#6 sample is 21.33 μm, and that of HT#4 and HT#5 samples is 34.82 and 39.82 μm, respectively. Hence, the reduction of the α_2/γ-colonies could contribute to microstructure refinement, thereby improving the strength of the alloy and correspondingly reducing the ductility.

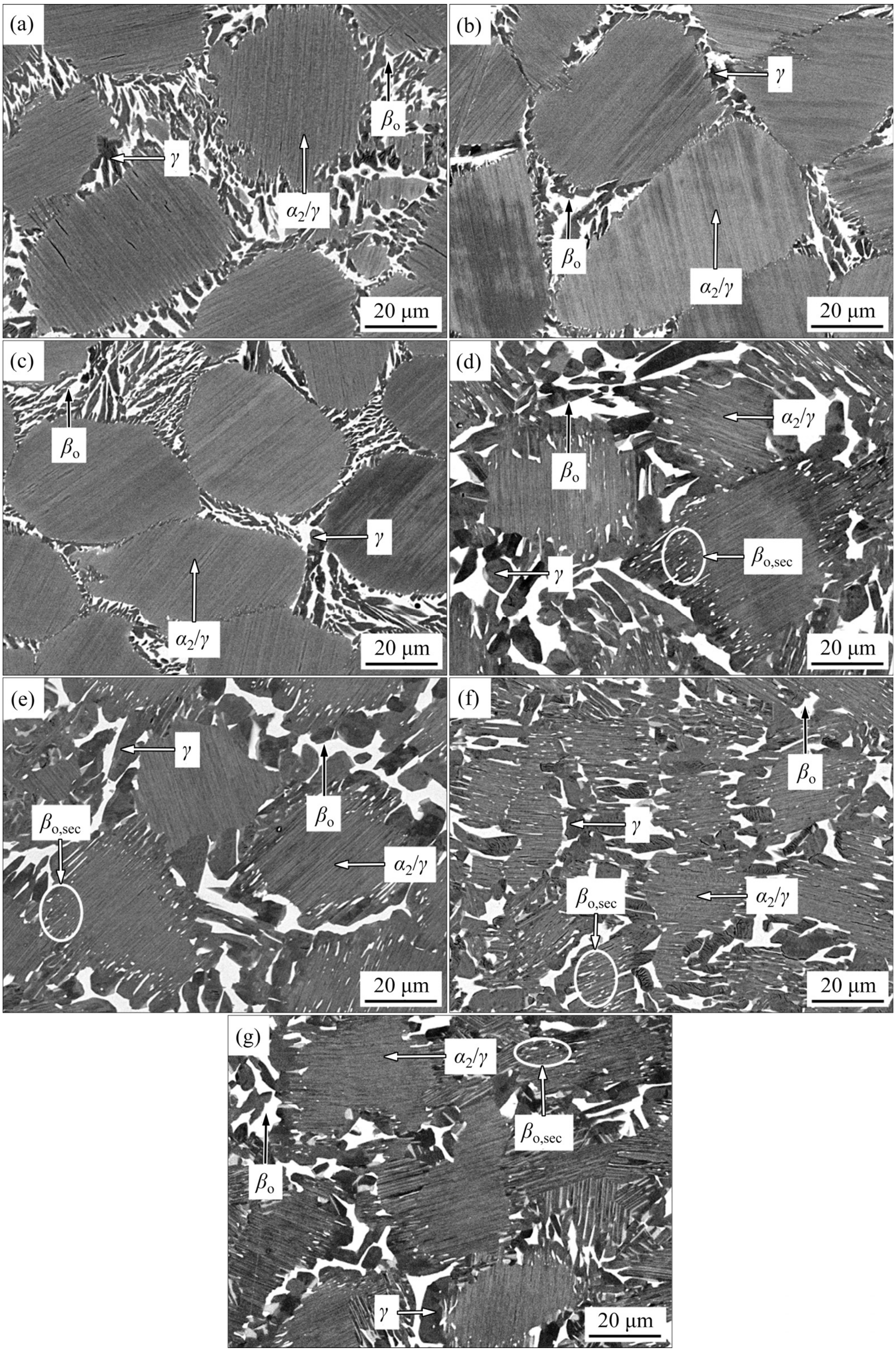

Fig. 8 Microstructures of as-forged Ti−42Al−5Mn alloy subjected to different heat treatments: (a) (1300 °C, 30 min, AC) + (800 °C, 3 h, FC); (b) (1275 °C, 30 min, AC) + (800 °C, 3 h, FC); (c) (1250 °C, 30 min, AC) + (800 °C, 3 h, FC); (d) (1300 °C, 30 min, AC) + (1000 °C, 3 h, FC); (e) (1275 °C, 30 min, AC) + (1000 °C, 3 h, FC); (f) (1250 °C, 30 min, AC) + (1000 °C, 3 h, FC); (g) (1275 °C, 10 min, AC) + (1000 °C, 3 h, FC)

Because the sizes of α_2/γ-colonies in HT#4 and HT#5 samples are approximately 35 μm, the strength difference between these two alloys is not obvious.

Compared with HT#5 with HT#7, it is found that, with the time reducing from 30 to 10 min, the volume fraction of γ grain decreases from 25.83%

Table 5 Microstructural parameters and tensile properties of as-forged alloys after subjecting to two-step heat treatments

HT	Phase fraction/%			Average size/μm		$R_{p0.2}$/MPa	R_m/MPa	A/%
	γ	β_o	α_2/γ	γ	α_2/γ-colony			
HT#1	12.64	9.38	77.98	3.05	36.35	515	566	0.20
HT#2	11.94	8.15	79.91	3.00	37.77	523	612	0.51
HT#3	12.29	8.84	78.87	3.12	36.57	515	565	0.19
HT#4	25.22	11.71	63.07	6.35	34.82	636	755	0.80
HT#5	25.83	12.62	61.55	6.40	34.92	649	758	0.79
HT#6	26.12	11.12	62.76	6.22	21.33	704	741	0.29
HT#7	21.11	11.33	67.56	5.23	31.68	735	794	0.55

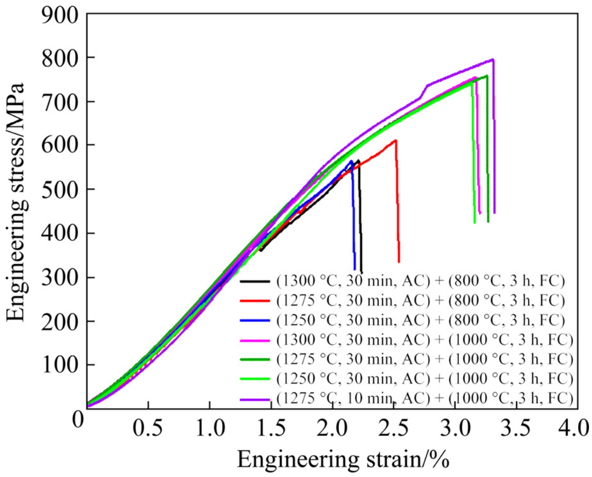

Fig. 9 RT tensile stress−strain curves of as-forged Ti−42Al−5Mn alloy subjected to different heat treatments

to 21.11%, and the size of γ grain reduces from 6.40 to 5.23 μm. Also, the size of α_2/γ lamellae decreases from 34.92 to 31.68 μm, and the volume fraction of β_o decreases from 12.62% to 11.33%. This indicates that the reduction of time will contribute to the microstructure refinement of this alloy, which is consistent with the results of Ref. [28]. Based on the tensile properties (see Table 5), the yield strength and tensile strength of HT#7 sample are both higher than that of HT#5 sample, but the elongation is lower. Combined with the previous analysis on HT#4 and HT#6 samples, it is found that the size of α_2/γ lamellae decreases from 34.82 (HT#4) to 21.33 μm (HT#6), and the yield strength of this alloy increases from 636 to 704 MPa, with an increment of 68 MPa. In the case of HT5# and HT7# samples, the α_2/γ lamellae size decreases from 34.92 to 31.68 μm, the yield strength of this alloy increases from 649 to 735 MPa with an increment of 86 MPa. Then it can be inferred that the reduction in the size of α_2/γ lamellae cannot be fully explained the increment of 86 MPa when the time reduces from 30 to 10 min. It is suggested that the increase in strength should be also induced by other factors. By comparison, for the HT#7 sample, it is found that the volume fraction of α_2/γ lamellae is increased (by about 6%), and the γ grain size is decreased to 5.23 μm. Therefore, the increase in the yield strength of this alloy should also be related to the higher fraction of α_2/γ lamellae and the lower size of γ grain.

4 Discussion

Ti−42Al−5Mn alloy is a typical beta solidified gamma alloys with the following solidification pathway from liquid to room temperature: $L\rightarrow L+\beta\rightarrow\beta\rightarrow\beta+\alpha\rightarrow\beta+\alpha+\gamma\rightarrow\beta_o+\alpha+\gamma\rightarrow\beta_o+\alpha_2+\gamma$ [24]. The present study has demonstrated that this alloy can be forged at 1300 °C by using conventional forging process without any isothermal or canned condition. However, the microstructure formed in the forging process is found to be thermodynamically unstable, namely the lamellar spacing and γ grain will be coarsened after exposure at 800 °C even for 3 h (see Table 2). It suggests that the structure obtained during the forging process is a non-equilibrium phase. This phenomenon has also been confirmed in some alloys. For instance, HUANG and ZHU [29] investigated the thermal stability of Ti−44Al−8Nb−1B alloy, and found that the fine-grained lamellar microstructure produced by ingot casting and hot-isostatic pressing would be unstable after exposure at 700 °C.

The present study has proved that the thermal stability of the forged alloy can be strongly improved by annealing treatment at 1300 °C. This treatment is aimed to ensure the α_2/γ lamellae and γ grain completely dissolved into the β phase. It is found that, for the alloy in this case, the α_2/γ lamellae and γ grain can completely dissolve into β-phases completely when the temperature is above $T_{\gamma,\text{solv}}$ (1250−1300 °C). The finer α_2/γ lamellae and γ grain could precipitate from β phase during the following air cooling process. Such structures would have a higher thermodynamic stability compared with the previous structures generated from forging. If the annealing treatment is conducted below $T_{\gamma,\text{solv}}$ (1100−1200 °C), there will be a significant increase in the volume fraction of γ grains and β_o phases. This is because when the temperature drops to the β+α+γ region, the γ phase cannot completely dissolve into β phase, and both the β_o phase and unresolved γ phase would be further coarsened during the annealing treatment. Particularly, the volume fraction of β_o phase is increased to ~25% (see Table 4). Combined with the Refs. [11,18,29,30], the β_o phase at colony boundary would induce the local stress concentration, which promotes the formation of globular structure and void, and could act as crack sources to accelerate its failure. Therefore, to achieve the low amount of β_o phase, the annealing temperature should be selected as 1250−1300 °C to ensure complete re-dissolution of these phases.

It should be mentioned that because Ti−42Al−5Mn is a typical BSG alloy, the volume fraction of β_o phase is still be as high as about 10% even for the 1250−1300 °C annealing samples. For these alloys, by a sufficient amount of β-stabilizing elements, their solidification behavior (via β phase) and the room temperature structure would be greatly affected. Previous research has proved that with the increase of β-stabilizing element content, the phase transformation would be as $\alpha_2+\gamma \rightarrow \beta+\alpha_2+\gamma \rightarrow \beta+\gamma$ [14,31,32]. Here the newly produced β is generated from α_2 phase, and when the β-stabilized elements are sufficient, the α_2 phase will transfer into β and γ phases, resulting in the new-precipitated β phases and thicker γ lath by the cellular reaction of $\alpha_2 \rightarrow \beta+\gamma$ [18]. SUN et al [11] established a relationship between the β phase and the contents of β-stabilizing elements, and concluded an empirical equation named as Cr equivalent. They found that if the Cr equivalent is more than 3.0, the β_o phase will form in microstructure. Based on the empirical equation, Mn is deemed as a strong β-stabilizing element which is similar to Cr, and about three times stronger than Nb. The Cr equivalent of Ti−42Al−5Mn alloy is up to 5.0, which is even larger than that of TNM alloy (3.0). Therefore, for the Ti−42Al−5Mn alloy, it is hard to completely remove the β_o phase just by heat treatments.

At these annealing temperatures (1250−1300 °C), a few supersaturated α_2-grain which is always considered as a non-equilibrium phase can be preserved during air cooling process (Figs. 7(a−c)). The following aging treatment is then used to promote the $\alpha_2 \rightarrow \gamma$ transformation; thereby the supersaturated α_2 phase can be transformed into fine lamellar spacing within the α_2/γ colonies. In this study, two different aging treatments (800 and 1000 °C) were considered. From Fig. 9, under the same annealing treatment, the strength and ductility of the specimens treated at 800 °C are generally lower than those of the 1000 °C aging specimens. Based on Table 5, it is found that the characteristics of α_2/γ lamellae, γ grain and β_o phase at colony boundary are different between the two aging treatments. As for α_2/γ lamellae, SCHWAIGHOFER et al [18] have proved that large fraction of α_2/γ colonies tends to have a strongly beneficial effect on the yield strength, which is detrimental to ductility. It can be seen that the volume fraction of α_2/γ colonies decreases from ~80% to ~60% with increasing aging temperature from 800 to 1000 °C. Based on the viewpoint of Ref. [18], the reduction of the lamellar structure tends to be detrimental to the strength of this alloy. Then the high strength of the 1000 °C aging alloy should be related to other factors.

Based on our previous research [26], the precipitation of $\beta_{\text{o,sec}}$ could occur below the eutectoid transformation temperature (T_eut), and it happens at 918−1024 °C cooled with 0.5 and 0.1 °C/s which is close to furnace cooling rate (FC≈ 20 °C/min [33]). As stated in Section 3.5, it is found that the 1000 °C aging process can induce the

$\alpha_2/\gamma \rightarrow \beta_{o,sec}$ transformation, then plenty of $\beta_{o,sec}$ phases are precipitated at lamellar interfaces, but it seems that none is formed during 800 °C aging. As for the $\beta_{o,sec}$, DU et al [34] proposed that the $\beta_{o,sec}$ precipitates in Ti−46.5Al−2Cr−3Nb−0.2W alloy always nucleated at α_2/γ colonies interfaces because W (β stabilizer) segregated in these areas. For Ti−42Al−5Mn, the precipitation of $\beta_{o,sec}$ could be mainly ascribed to the strong segregation of β-stabilizing element Mn at lamellar colony. As confirmed in the previous results [35−37], the fine $\beta_{o,sec}$ generated during the heat treatment could improve the fracture toughness and creep strength of γ-TiAl alloys. Therefore, it is believed that the presence of fine $\beta_{o,sec}$ will be an important reason for the strength improvement of this alloy.

In addition, related literature [26] suggested that the γ phase at colony boundary was a ductile phase, and can improve the ductility of the γ-TiAl alloy. For the as-forged Ti−42Al−5Mn, when it was annealed at 1250−1300 °C first and then aged at 800 °C, the obtained γ grain would be as small as ~3 μm. While for 1000 °C aging, the size of γ grain is ~6 μm which is about two times as large as that of 800 °C aging. In this study, it can be seen that the microstructure containing small size γ grains (~3 μm) fails to improve the ductility of this alloy. On the contrary, the microstructure containing larger size γ grains (~6 μm) has positive effect on its ductility. Hence, it confirms that in order to obtain an alloy with better ductility, the size control of γ phase is an important factor in the regulation of the microstructure, and a smaller γ phase size (eg, ~3 μm) does not function well for plasticity improvement.

5 Conclusions

(1) The microstructure of the forged Ti−42Al−5Mn alloy was characterized to be instability when it was aged 800 °C for 24 h.

(2) The high temperature treatment can stabilize the forged microstructure, and the suggested temperature range is 1250−1300 °C which is in the $\beta+\alpha$ region.

(3) Combined with the annealing treatment at 1250−1300 °C, the 1000 °C aging process makes the as-forged Ti−42Al−5Mn alloy have better strength and ductility than those of 800 °C aging process.

(4) $\beta_{o,sec}$ precipitates generated along lamellar colony boundaries by the 1000 °C aging treatment could be responsible for strength improvement, and the better ductility would be mainly due to the suitable γ phase size, which is believed to be about 6 μm.

Acknowledgments

The authors thank the Jihua Laboratory Scientific Research Project, China (No. X210291TL210), the National Natural Science Foundation of China (No. 51971215), and the Natural Science Foundation of Liaoning Province of China (No. 2019-MS-330).

References

[1] APPEL F, WAGNER R. Microstructure and deformation of two-phase γ-titanium aluminides [J]. Materials Science and Engineering R, 1998, 22: 187−268.

[2] CLEMENS H, KESTLER H. Processing and applications of intermetallic γ-TiAl-based alloys [J]. Advanced Engineering Materials, 2000, 2: 551−570.

[3] YAMAGUCHI M, INUI H, ITO K. High-temperature structural intermetallics [J]. Acta Materialia, 2000, 48: 307−322.

[4] LI Y, ZHOU L, LIN J P, CHANG H, LI F. Phase transformation behavior and kinetics of high Nb−TiAl alloy during continuous cooling [J]. Journal of Alloys and Compounds, 2016, 668: 22−26.

[5] IMAYEV V, OLENEVA T, IMAYEV R, CHRIST H J, FECHT H J. Microstructure and mechanical properties of low and heavy alloyed γ-TiAl+α_2-Ti_3Al based alloys subjected to different treatments [J]. Intermetallics, 2012, 26: 91−97.

[6] GAO Guo-fu, FU Zong-xia, WANG Yi, XIANG Dao-hui, ZHAO Bo. Research progress on precision machining of Ti−Al intermetallic compounds [J]. Rare Metal Materials and Engineering, 2021, 50(5): 1867−1882.

[7] NAKA S, NATHAL M V, DAROLIA R, LIU C T, MARTIN P L, MIRACLE D B, WAGNER R, YAMAGUCHI M. Structural intermetallics [M]. Warrendale, PA: TMS, 1997: 313.

[8] KIM Y W, KIM S L. Advances in gammalloy materials–processes–application technology: Successes, dilemmas, and future [J]. JOM, 2018, 70: 553−560.

[9] XU Run-run, LI Miao-quan. Quantitative characterization of β-solidifying γ-TiAl alloy with duplex structure [J]. Transactions of Nonferrous Metals Society of China, 2021, 31: 1993−2004.

[10] YANG J R, XIAO B, HAN P, KOU H C, LI J S. Microstructure evolution in the mushy zone of a

β-solidifying TiAl alloy under different cooling processes [J]. Advanced Engineering Materials, 2016, 18: 1667−1673.

[11] SUN F S, CAO C X, YAN M G, KIM S E, LEE Y T. Alloying mechanism of beta stabilizers in a TiAl alloy [J]. Metallurgical and Materials Transactions A, 2001, 32: 1573−1589.

[12] TETSUI T, SHINDO K, KOBAYASHI S, TAKEYAMA M. A newly developed hot worked TiAl alloy for blades and structural components [J]. Scripta Materialia, 2002, 47: 399−403.

[13] CLEMENS H, CHLADIL H F, WALLGRAM W, ZICKLER G A, GERLING R, LISS K D, KREMMER S, GÜTHER V, SMARSLY W. In and ex situ investigations of the β-phase in a Nb and Mo containing γ-TiAl based alloy [J]. Intermetallics, 2008, 16: 827−833.

[14] SCHMOELZER T, MAYER S, SAILER C, HAUPT F, GÜTHER V, STARON P, LISS K D, CLEMENS H. In situ diffraction experiments for the investigation of phase fractions and ordering temperatures in Ti−44at.%Al−(3−7)at.%Mo alloys [J]. Advanced Engineering Materials, 2011, 13: 306−311.

[15] XU X J, LIN J P, TENG Z K, WANG Y L, CHEN G L. On the microsegregation of Ti−45Al−(8−9)Nb−(W, B, Y) alloy [J]. Materials Letters, 2007, 61: 369−373.

[16] SCHMOELZER T, LISS K D, ZICKLER G A, WATSON I J, DROESSLER L M, WALLGRAM W, BUSLAPS T, STUDER A, CLEMENS H. Phase fractions, transition and ordering temperatures in TiAl−Nb−Mo alloys: An in-and ex-situ study [J]. Intermetallics, 2010, 18: 1544−1552.

[17] BUTLER C J, MCCARTNEY D G, SMALL C J, HORROCKS F J, SAUNDERS N. Solidification microstructures and calculated phase equilibria in the Ti−Al−Mn system [J]. Acta Materialia, 1997, 45: 2931−2947.

[18] SCHWAIGHOFER E, CLEMENS H, MAYER S, LINDEMANN J, KLOSE J, SMARSLY W, GÜTHER V. Microstructural design and mechanical properties of a cast and heat-treated intermetallic multi-phase γ-TiAl based alloy [J]. Intermetallics, 2014, 44: 128−140.

[19] BOLZ S, OEHRING M, LINDEMANN J, PYCZAK F, PAUL J, STARK A, LIPPMANN T, SCHRÜFER S, ROTH-FAGARASEANU D, SCHREYER A, WEIß S. Microstructure and mechanical properties of a forged β-solidifying γ TiAl alloy in different heat treatment conditions [J]. Intermetallics, 2015, 58: 71−83.

[20] XU H, LI X B, XING W W, SHU L, MA Y C, LIU K. Processing map and hot working mechanism of as-cast Ti−42Al−5Mn alloy [J]. Advanced Engineering Materials, 2018, 20(6): 1701059.

[21] SCHWAIGHOFER E, CLEMENS H, LINDEMANN J, STARK A, MAYER S. Hot-working behavior of an advanced intermetallic multi-phase γ-TiAl based alloy [J]. Materials Science and Engineering A, 2014, 614: 297−310.

[22] JIANG H T, ZENG S W, ZHAO A M, DING X N, DONG P. Hot deformation behavior of β phase containing γ-TiAl alloy [J]. Materials Science and Engineering A, 2016, 661: 160−167.

[23] LI X B, TANG H J, XING W W, ZHAO P X, CHEN B, MA Y C, LIU K. Microstructural stability, phase evolution and mechanical properties of a forged W-modified high-Mn β-γ-TiAl alloy [J]. Intermetallics, 2021, 136: 107230.

[24] XU H, LI X B, XING W W, SHU L, MA Y C, LIU K. Solidification pathway and phase transformation behavior in a beta-solidified gamma-TiAl based alloy [J]. Journal of Materials Science & Technology, 2019, 35(11): 2652−2657.

[25] CHENG Liang, ZHANG Shuai-jin, YANG Guang, KOU Hong-chao, BOUZY E. Tailoring microstructure and mechanical performance of a β-solidifying TiAl alloy via martensitic transformation [J]. Materials Characterization, 2021, 173: 110970.

[26] XU H, LI X B, XING W W, SHU L, MA Y C, LIU K. Phase transformation behavior of a Mn containing β-solidifying γ-TiAl alloy during continuous cooling [J]. Intermetallics, 2018, 99: 51−58.

[27] MAYER S, ERDELY P, FISCHER F D, HOLEC D, KASTENHUBER M, KLEIN T, CLEMENS H. Intermetallic β-solidifying γ-TiAl based alloys−from fundamental research to application [J]. Advanced Engineering Materials, 2017, 19: 1600735.

[28] SCHLOFFER M, IQBAL F, GABRISCH H, SCHWAIGHOFER E, SCHIMANSKY F P, MAYER S, STARK A, LIPPMANN T, GÖKEN M, PYCZAK F, CLEMENS H. Microstructure development and hardness of a powder metallurgical multi phase γ-TiAl based alloy [J]. Intermetallics, 2012, 22: 231−240.

[29] HUANG Z W, ZHU D G. Thermal stability of Ti−44Al−8Nb−1B alloy [J]. Intermetallics, 2008, 16: 156−167.

[30] WANG Q, CHEN R R, YANG Y H, WU S P, GUO J J, DING H S, SU Y Q, FU H Z. Effects of lamellar spacing on microstructural stability and creep properties in β-solidifying γ-TiAl alloy by directional solidification [J]. Materials Science and Engineering A, 2018, 711: 508−514.

[31] FANG H Z, CHEN R R, GONG X, SU Y Q, DING H S, GUO J J, FU H Z. Effects of Nb on microstructure and mechanical properties of $Ti_{42}Al_{2.6}C$ alloys [J]. Advanced Engineering Materials, 2018, 20(4): 1701112.

[32] CHEN G L, XU X J, TENG Z K, WANG Y L, LIN J P. Microsegregation in high Nb containing TiAl alloy ingots beyond laboratory scale [J]. Intermetallics, 2007, 15: 625−631.

[33] ZHU H L, SEO D Y, MARUYAMA K. Strengthening behavior of beta phase in lamellar microstructure of TiAl alloys [J]. JOM, 2010, 62: 64−69.

[34] DU X W, ZHU J, ZHANG X, CHENG Z Y, KIM Y W. Creep induced $\alpha_2\rightarrow\beta_2$ phase transformation in a fully-lamellar TiAl alloy [J]. Scripta Materialia, 2000, 43: 597−602.

[35] KIM Y W. Ordered intermetallic alloys, part III: Gamma titanium aluminides [J]. JOM, 1994, 46: 30−39.

[36] DU X W, ZHU J, ZHANG X, CHENG Z Y, KIM Y W. Formation of the creep-induced β_2 phase and its influence on deformation in a fully-lamellar TiAl alloy [J]. Intermetallics, 2001, 9: 181−187.

[37] KIM Y W, KIM S L. Effects of microstructure and C and Si additions on elevated temperature creep and fatigue of gamma TiAl alloys [J]. Intermetallics, 2014, 53: 92−101.

热处理对锻造 β 凝固 γ-TiAl 合金组织演变与力学性能的影响

李小兵[1]，许 昊[2]，邢炜伟[3]，陈 波[1]，舒 磊[1]，张孟殊[1]，刘 奎[1]

1. 季华实验室(先进制造科学与技术广东省实验室)，佛山 528200；
2. 南京理工大学 工信部先进金属及金属间化合物材料技术重点实验室，南京 210094；
3. 中国科学院 金属研究所 师昌绪先进材料创新中心，沈阳 110016

摘 要：研究不同热处理制度锻态 Ti−42Al−5Mn 合金的组织和拉伸性能演变行为。结果表明，当锻态合金在 800 ℃时效 24 h 时，片层间距和 γ 相晶粒尺寸均增加。而经 1300 ℃处理，然后在 800 ℃时效 24 h 时，合金片层间距和 γ 相晶粒尺寸变化不大，由此获得合金理想的高温处理温度区间 1250~1300 ℃，处于 β+α 区。在该最佳高温处理温度区间 1250~1300 ℃处理后再经 1000 ℃时效处理，合金的强度和塑性均优于同样高温处理后再经 800 ℃时效处理的合金。1000 ℃时效处理在片层组织晶团界面处诱发析出的 $\beta_{o,sec}$ 相是合金强度提高的重要原因，而片层组织晶团界面处析出的~6 μm γ 相晶粒是合金更高塑性的主要原因。

关键词：β 凝固 γ-TiAl 合金；锻造；热处理；组织演变；力学性能

(Edited by Xiang-qun LI)